Vessel tree extraction and depth estimation with OCT images

Joaquim de Moura[1], Jorge Novo[1], Marcos Ortega[1], Noelia Barreira[1], Manuel G. Penedo[1]
{joaquim.demoura,jnovo,mortega,nbarreira, mgpenedo}@udc.es

Departamento de Computación. Universidade da Coruña, A Coruña (Spain)

Abstract. The identification of the retinal arterio-venular tree is a relevant issue for its analysis in a large variability of procedures. Classical methodologies employ 2D acquisition strategies that obtain a limited representation of the vascular structure. This paper proposes a new methodology for 2D vessel tree extraction and the corresponding depth estimation using Optical Coherence Tomography (OCT) images. This way, the proposal defines a more complete scenario for an adequate posterior vasculature analysis. The methodology employs different image analysis techniques to initially extract the 2D vessel tree. Then, the method maps these 2D positions in the corresponding histological sections of the OCT images and estimates the corresponding depths along all the vessel tree. To test and validate this proposal, this work employed 196 OCT histological images with the corresponding near infrared reflectance retinographies. The methodology provided promising results, indicating an acceptable accuracy in a complex domain as is the vessel tree identification. It provides a coherent 2D vessel tree extraction with the corresponding depth estimations that constitute a scenario with high potentially useful information for posterior medical analysis and diagnostic processes of many diseases as, for example, hypertension or diabetes.

Keywords: Computer-aided diagnosis, retinal imaging, OCT, vessel tree.

1 Introduction and previous work

Eye fundus is, nowadays, a frequently used way of analyzing and diagnosing many different diseases. The study of retinal images provides the doctors useful information that can be of a great utility to obtain accurate diagnosis in a large variability of pathologies. In these diagnostic procedures, Computer-Aided Diagnostic (CAD) systems have demonstrated its utility as many different approaches. These computational approaches help the doctors to increase their productivity, minimize the risks of possible mistakes and help to establish preventive and therapeutic strategies.

CAD systems for the identification and analysis of the eye fundus main structures were appearing over the years. The vessel tree extraction is one of the most relevant issues, as its analysis is fundamental for the microcirculation analysis due to the fact that the retinal microcirculation is the easiest and less invasive

way to access to the circulatory system in human body. Different studies arised over the years stating this relevance. For example, the vessel caliber was demonstrated to be a parameter of high relevance in the analysis of diabetic patients [1]. Others indicated that the microcirculation constitute a relevant biomarker for cerebrovascular diseases [2] or cardiovascular illnesses [3].

The task of vessel tree extraction was faced by different authors over the years, and interesting methodologies were appearing. Despite that, most of them proposed segmentation methodologies for 2D vessel tree segmentation using angiographies or retinographies, image modalities that provide 2D projections of the real 3D layout of the vasculature. We include a representative set of proposed methodologies as illustration.

Thresholding approaches were employed in this issue. Hence, Zhang *et al.* [4] or Yong *et al.* [5] designed adaptative thresholding processes to extract the vessel tree in retinographies. Tracking approaches also demonstrated its utility as the work of Wink *et al.* [6], who implemented a methodology that begins from a set of user-defined image coordinates and provides the central axis of tubular structures, as is the case of the retinal vasculature. Edge detectors were also used, as the work of Dhar *et al.* [7] testing Canny and Laplacian of gaussian detectors. The authors stated that Canny is more robust in these particular image conditions. Region growing approaches were also proposed, as the work of Mendonça and Campilho [8] that proposed a method that firstly extracts the vessel centerline and then uses a region growing process to fill the extracted vessels. Wavelet transform was also included in different proposals as the one of Fathi *et al.* [9] where information over multiple classification scales was integrated to obtain the vessels.

Regarding Optical Coherence Tomography (OCT) images, few works appeared for vessel extraction. Wu *et al.* [10] proposed a methodology that uses Point Drift to obtain the retinal vessel point sets. Then, this set is used as landmarks for image registration. Niemeijer08 *et al.* [11] proposed a method that segments the retina in multiple layers performing a posterior classification in the projected image to extract the vessels. In the work of Xu *et al.* [12] a 3D boosting learning approach is employed for vessels detection. Then, a post-processing step is done to remove false positive detections.

Given the high potential of a 3D analysis of the vessel tree, we present in this work a new methodology to identify the vessel tree in OCT images. The method firstly extracts the 2D vessel tree that is posteriorly mapped with the corresponding histological sections. Finally, the corresponding depth coordinates are estimated for each detected vessel point. This way, this proposal offers a methodology that provides a more complete information set of the retinal arterio-venular tree that could facilitate further and more precise retinal microcirculation analysis than simple 2D extractions.

2 Methodology

The proposed methodology makes use of, as input, the OCT image. The OCT imaging technique let us obtain tomographic images of the biological tissue with

high resolution, performing consecutive measurements, the histological sections, that provide the depth at the progressive bands over the eye fundus. Hence, these consecutive histological sections compose the 3D representation of the eye fundus of the patient. This 3D visualization is complemented with the corresponding near infrared reflectance retinography, automatically registered with the histological sections, that offer a classical 2D visualization of the corresponding eye fundus region where the histological section were obtained. Figure 1 includes a illustrative example of an OCT image. The input images include the representation of the region of interest (ROI), region that indicates the part of the retinography that is mapped with the histological sections. Both are the parts where we can search and analyze the retinal vessel tree of a patient.

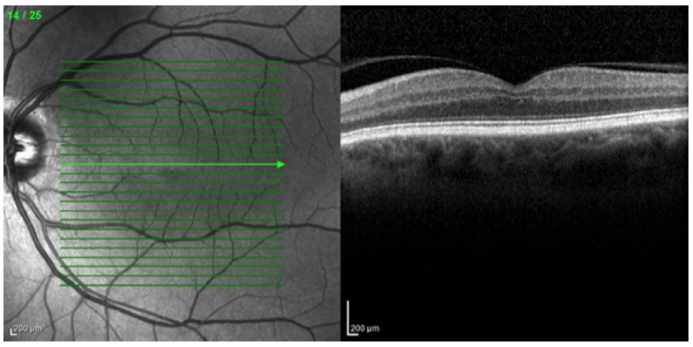

Fig. 1. Near infrared reflectance retinography and histological section example.

The new approach is mainly composed of three consecutive stages: a first one, where the vessel tree is extracted in the near infrared reflectance retinography, providing a 2D vasculature extraction; a second one, where this initial 2D identifications are mapped in the corresponding histological sections; and a third one, where the approach searches for the vessel location in the histological sections and derives the corresponding depth positions at the mapped points. This process is performed over the entire vessel tree obtaining, finally, a complete set of (x, y, z) coordinates over all the vasculature. Next subsections detail the process.

2.1 2D vessel tree extraction

As said, we firstly segment the vessels in the 2D near infrared retinography for its simplicity and given that there is well-established techniques to achieve that. In particular, a segmentation process based in morphological operators [13] is used to enhance the vessels and identify an initial vessel representation.

The vessel enhancement stage employs a multi-scalar approach where the eigenvalues, λ_1 and λ_2, of the Hessian matrix [14] are combined to filter geometric tubular structures with variable size, that is, the vessels. Thus, a function $B(p)$ is defined as:

$$B(p) = \begin{cases} 0 & \lambda_2 > 0 \\ exp(\frac{-R_B^2}{2_\beta^2})(1 - exp(-\frac{S^2}{2c^2})) & otherwise \end{cases} \quad (1)$$

where $R_b = \lambda_1/\lambda_2$, c is the half of the max Hessian norm, S represents a measure to "second order structures". Pixels that belongs to vessels are normally represented by small λ_1 values and higher positive λ_2 values. After this enhancement, the vascular segmentation is achieved in two steps: an early segmentation and a posterior removal of isolated structures. The early segmentation is done by a hysteresis based thresholding. A hard threshold (T_h) obtain pixels with a high confidence of being vessels while a weak threshold (T_w) keeps all the pixels of the tree, including also spurious ones. The final vessel segmentation is formed by all the pixels included by T_w that are connected to, at least, one pixel obtained by T_h.

Segmentation approaches in 2D can not be directly used for reconstruction as they typically present cumulative errors due to misrepresentation of the edges. This way, a centerline-based approach is normally used to correct deviation in the detected structure. The main purpose of this stage is the identification of the approximate central line of the vessels in order to obtain a set of consecutive coordinates that represents all the vasculature. This process is performed with an approach that exploits the concept that vessels can be thought of as creases (ridges or valleys) when images are seen as landscapes. Hence, curvature level curves are used to calculate the creases (crest and valley lines).

As definition of a crease, this proposal implemented a level set extrinsic curvature or LSEC, Eq. 2, given its invariant properties. This approach segment the vessel tree that is going to be 2D structure of the identified vessel tree. Given a function $L : \mathbb{R}^d \to \mathbb{R}$, the level set for a constant l consists of the set of points $x|L(x) = l$. For 2D images, L can be considered as a topographic relief or landscape and the level sets as its level curves. Negative minima of the level curve curvature k, level by level, form valley curves, and positive maxima form ridge curves.

$$k = (2L_xL_yL_{xy} - L_y^2L_{xx} - L_x^2L_{yy})(L_x^2 + L_y^2)^{-\frac{3}{2}} \quad (2)$$

where

$$L_\alpha = \frac{\partial L}{\partial \alpha}, L_{\alpha\beta} = \frac{\partial^2 L}{\partial \alpha\, \partial \beta}, \alpha, \beta \in x, y \quad (3)$$

However, the usual discretization of LSEC is ill-defined in a number of cases, giving rise to unexpected discontinuities at the centre of elongated objects. Due to this, the Multilocal Level Set Extrinsic Curvature with Structure Tensor, MLSEC-ST operator, originally defined [15] for 3D landmark extraction of CT and MRI volumes, is used:

$$k = -div(\bar{w}) = -\sum_{i=1}^{d}(\frac{\partial \bar{w}^i}{\partial x^i}), d = 2; \quad (4)$$

where $\bar{w}^i$ is the component at the position i of $\bar{w}$, the normalized vector field of $L : \mathbb{R}^d \to \mathbb{R}$. This last is defined by Eq. 5, where O_d is the d-dimensional zero vector.

$$\bar{w} = \begin{cases} \frac{w}{\|w\|}, \, if \, \|w\| > 0 \\ O_d, \, if \, \|w\| = 0 \end{cases} \tag{5}$$

This work does not face the extraction of the caliber of the vessel tree, just a 3D coordinate representation of the entire points of the vasculature. The employed crease method does not return a 1-pixel width segment as there are degrees of creaseness along the vessel. For that reason, all the pixels are labeled with a tracking process that checks all the crease image and guarantees that all the detected pixels are grouped belonging to a particular vessel. The aim of this process is the obtaining of a skeleton vessel tree structure with all the vessels represented by one-pixel width segments. Moreover, small detected vessels are removed considering that belong to detections of different structures than vessels as noisy artifacts in the image. This way, this process offers the detection of the (x, y) coordinates for the entire vessel tree. Examples of this process can be seen in Figure 2 where the original image, 2D vessel tree extraction and skeletonization are included in Figures 2 (a), (b) and (c), respectively.

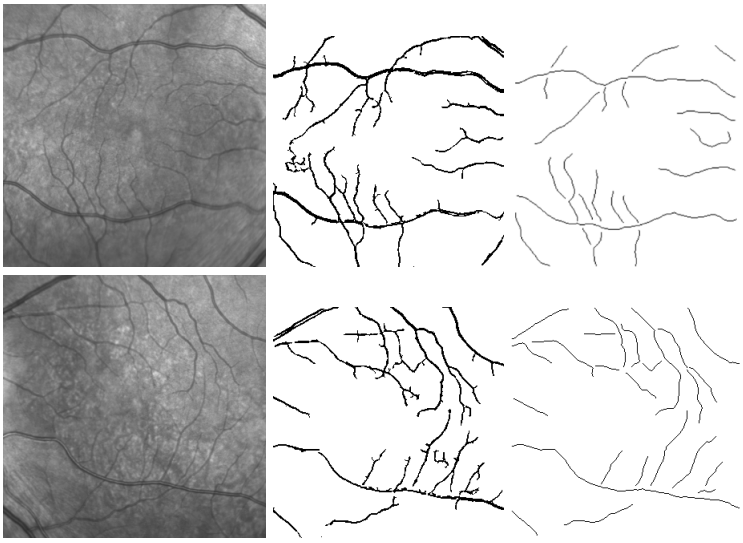

(a) (b) (c)

Fig. 2. 2D vessel tree extraction and skeletonization.(a) Input retinography.(b) 2D Vessel tree extraction.(c) Skeletonized vessel tree.

2.2 Vessel coordinates mapping in the histological sections

Once the (x, y) coordinates of the vasculature is detected, we need to calculate the corresponding depth, or z, at all these detected points. The depth can be

obtained with the OCT scans, as the histological sections provide the depth information over the entire eye fundus analyzed region. In the histological sections, the vessels are visualized as structures that blocks the transmission of light, leaving a shadow and revealing, therefore, its location. This can be seen in Figure 3(a), where a histological section with the presence of several vessels is presented. As we know, each histological section corresponds to a band in the 2D retinography. We can identify in the intersection of the band and the 2D vessel tree the vessel positions that appear in this particular band visualized in the histological section.

Therefore, we analyze all the bands that correspond with the histological sections and identify all the vessel points that intersect with the band. This way we can map all the 2D coordinates of the vasculature that are present in the histological sections, identifying their projection zones, that is, the region that corresponds with each vessel shadow. This process is illustrated in Figure 3(b), where this mapping process can be clearly seen. In these projection zones, we can posteriorly identify the depth at which each vasculature points is located.

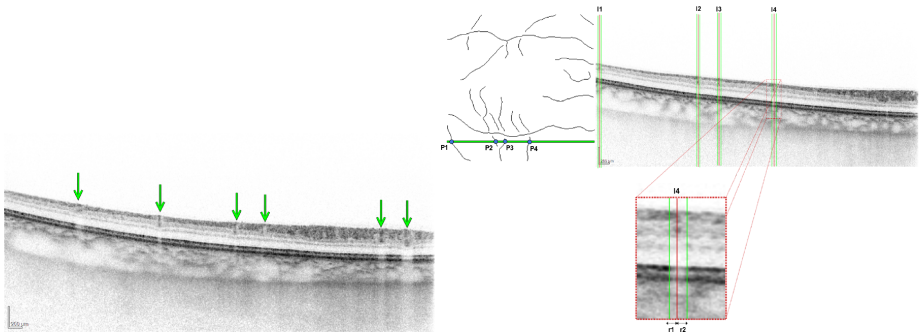

(a) (b)

Fig. 3. Vasculature coordinates mapping in the corresponding histological sections process. (a) Example of histological section with the shadow projection of a set of vessels clearly visible. (b) Example of mapping process, identifying the projection zones of a set of vasculature coordinates.

2.3 Depth vasculature estimation

Once we mapped the vasculature in the histological sections, We can obtain the corresponding depth coordinates z for each vasculature position. Hence, we can search in the mapped region a dark structure that produce a shadow, as commented before. This process is performed in two consecutive steps.

ILM and RPE layers identification In the histological sections, the vessels can only appear between the retinal layers Inner Limitant Membrane (ILM), the first intraretinal layer, and the Retinal Pigment Epithelium (RPE), formed by pigmented cells at the external part of the retina. Taking advantage of this, we can reduce the search space to the region between those layers, minimizing the risk of possible miscalculations.

We employed the Canny edge detector to find where these layers are placed considering that both ILM and RPE layers contain the edges with the highest contrast of intensities among all the layers. Firstly, we apply the gradient to the image in the horizontal direction to gain information, producing strongest detections and guaranteeing that both layers are correctly obtained. In this resultant image, the upper and lower connected lines of these edges identify the limits of the ILM and RPE layers, respectively. An example of this process is shown in Figure 4(a).

Vessel point depth detection In this reduced search space, each vessel coordinates can be clearly searched, appearing as a small dark elliptic region, due to its particular reflectance properties compared to retinal layers. Firstly, a mean filter with a window of 3×3 is applied to smooth the ROI and avoid noisy detections. Then, the darkest spot inside the region of interest is identified as the vessel location. This is illustrated in Figure 4(b). Finally the depth value is derived by taking RPE layer lower limit as baseline and computing the height of the vessel center related to the baseline:

$$z = |C_v - P_i| \tag{6}$$

where z is the distance that measure the depth value, C_v indicates the y coordinate of the center of the detected vessel in the histological image, and P_i indicates the y coordinate of the lower limit of the RPE layer.

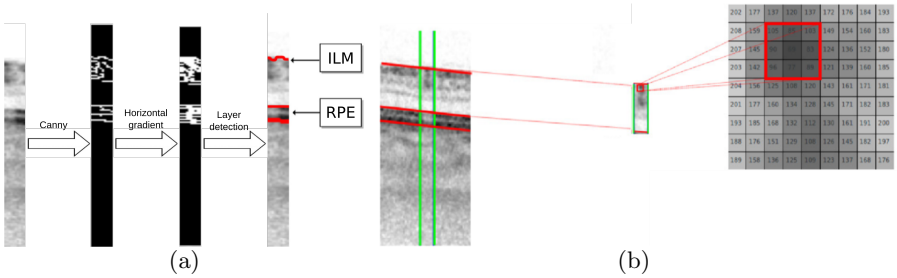

Fig. 4. Vessel depth identification process. (a) Detection of ILM and RPE layers. (b) Detection of the vessel in the search region.

3 Results

The implemented methodology was tested with a dataset of 196 OCT histological images that were taken with a confocal scanning laser ophtalmoscope, a CIRRUS^{TM}HD-OCT–Carl Zeiss Meditec. This OCT images also provided the corresponding near infrared reflectance retinographies. All the scans are centered in the macula and were obtained from both left and right eyes. The images have a resolution of 1520×496 pixels. For all the tests, the groundtruths were constructed in the collaboration with an expert of the field.

Vessel coordinates mapping in the histological sections. After the 2D vessel tree detection, we tested the accuracy of the vasculature mapping in

Table 1. Results obtained at the different stages of the methodology.

	Vessel mapping in OCT	**Depth calculation**
correctly processed	525	641
Test set size	607	704
Success rate	86,49%	91,05%

the corresponding histological sections. From the entire dataset, we randomly selected a set of vessel points, calculate their corresponding mappings and measure if this process was correctly performed. In particular a set of 607 points were analyzed obtaining a success rate of 86,49%, as shown in Table 1.

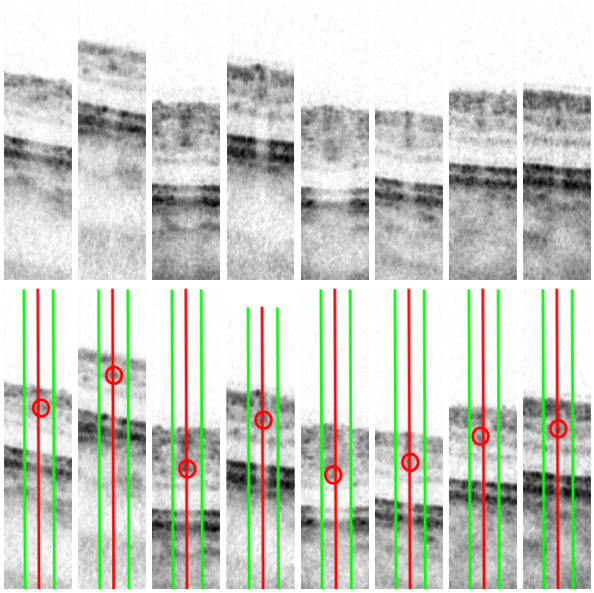

Fig. 5. Examples of correct vessel depth identifications. 1^{st} row, vessels to locate. 2^{nd} row, obtained detections.

Depth vasculature estimation. We also tested the method to identify the location of the vessel inside the histological sections and the adequate estimation of the depth position with respect to the RPE layer lower limit. In this particular case, we consider a success if, after a correct mapping of a vessel, the method identifies correctly the dark spot that belongs to the vessel and also, if the RPE layer was correctly identified, as it is a necessary condition to derive the depth of the vessel. This stage was tested with a constructed set of 704 annoted vessels that were randomly selected from the entire dataset. Table 1 shows a success rate of 91,95%, demonstrating the accuracy of the implemented approach.

Figure 5 presents 8 cases of correct vessel mapping and identification in the corresponding histological sections, detecting in all the cases the darkest spot in the search space that belong to the vessels. We also present some wrong detections in Figure 6. In this particular cases, the method finds the darkest spot between the ILM and RPE layers but belong to noisy artifacts or overlapped vessels instead of the desired one. Normally incorrect detections are mainly due to: (1) noisy artifacts or vessels that are too close and appear in the same region of the histological section as the objective vessel position; (2) alterations of a particular layer that can produce dark regions that can be confused with a vessel; (3) impossibility of detecting the dark spot of a vessel, as sometimes vessels can be parallel to the histological section, without producing the typical dark spot of a vessel intersection.

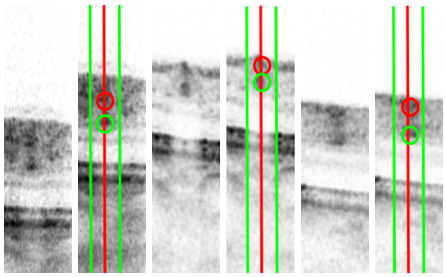

Fig. 6. Examples of wrong vessel depth identifications. 1^{st} row, vessels to locate. 2^{nd} row, results: red circle, the obtained vessel location: green circle, real vessel location.

4 Conclusions

This paper presented a new methodology for arterio-venular tree extraction and depth estimation using OCT images. The method provides the combination of the 2D vasculature structure extraction, done in the infrared reflectance retinographies, with their corresponding depth estimation over the positions of the entire vessel tree, thanks to the depth information that the histological sections provide. This way, we finally obtain the entire set of (x, y, z) coordinates over the entire arterio-venous tree. Thanks to that, doctors are provided with a more complete information set, instead of classical 2D vessel segmentations, to be able to do further analysis of the retinal microcirculation that constitute a key analysis for the assessment of several prevalent conditions such as hypertension, diabetes or cardiovascular risk.

Key stages of the approach were tested with a set of 196 OCT histological sections and the corresponding near infrared reflectance retinographies, showing promising results.

In future works, we plan to improve each of the stages of the method, trying to overcome some of the identified drawbacks of the issue and, therefore, increase the success rates that were obtained. Larger datasets will be also analyzed, in order to reinforce the conclusions that were achieved.

Acknowledgments This work is supported by the Instituto de Salud Carlos III, Government of Spain and FEDER funds of the European Union through the PI14/02161 and the DTS15/00153 research projects and by the Ministerio de Economía y Competitividad, Government of Spain through the DPI2015-69948-R research project.

References

1. Nguyen, T. T., Wang, J. J., Sharrett, A. R. et al. Relationship of retinal vascular caliber with diabetes and retinopathy: The multi-ethnic study of atherosclerosis (MESA). *Diabetes Care Journal*, 31(3):544–549, 2007.
2. Smith, W., Wang, J. J., Wong, T. Y. et al. Retinal arteriolar narrowing is associated with 5-year incident severe hypertension: The blue mountains eye study. *Hypertension Journal*, 44(4):442–447, 2004.
3. Wong, T.Y. Quantitative retinal venular caliber and risk of cardiovascular disease in older persons. *Archives of Internal Medicine Journal*, 166(21):2388–2394, 2006.
4. Zhang, Y., Hsu, W., Lee, M.L. Segmentation of retinal blood vessels by combining the detection of centerlines and morphological reconstruction. *Journal of Signal Processing Systems*, 55(1):103–112, 2008.
5. Yong, Y., Yuan, Z., Shuying, H. et al. Effective combined algorithms for retinal blood vessels extraction. *Advances in Information Sciences and Service Sciences Journal*, 4(3):263–269, 2012.
6. Wink, O., Niessen, W.J., and Viergever, M.A. Adaptive local thresholding by verification-based multithreshold probing with application to vessel detection in retinal images. *IEEE Transactions on Medical Imaging*, 23(1):130–133, 2004.
7. Dhar, R., Gupta, R., Baishnab, K.L. An analysis of canny and laplacian of gaussian image filters in regard to evaluating retinal image. *Int. Conference on Green Computing Communication and Electrical Engineering*, 31(8):1–6, 2014.
8. Mendonça, A.M., Campilho, A. Segmentation of retinal blood vessels by combining the detection of centerlines and morphological reconstruction. *IEEE Trans. Med. Imaging*, 25(9):1200–1213, 2006.
9. Fathi, A., Naghsh, N., Reza, A. Blood vessels segmentation in retina: Preliminary assessment of the mathematical morphology and of the wavelet transform techniques. *Biomedical Signal Processing and Control Journal*, 8(1):71–80, 2013.
10. Wu, J., Gerendas, B., Waldstein, S. et al. Stable registration of pathological 3D-OCT scans using retinal vessels. *Proc. Ophtalmic Medical Image Analysis.*, 2014.
11. Niemeijer, M., Garvin, M.K., van Ginneken, B., Sonka, M., Abrámoff, M.D. Vessel segmentation in 3D spectral OCT scans of the retina. *SPIE proceedings*, 2008.
12. Xu, J., Tolliver, D.A., Ishikawa, H., Wollstein, G., Schuman, J.S. 3D OCT retinal vessel segmentation based on boosting learning. *Medical Image Analysis*, 25(11):179–182, 2009.
13. Calvo, D., Ortega, M., Penedo, M.G., Rouco, J. Automatic detection and characterisation of retinal vessel tree bifurcations and crossovers in eye fundus images. *Computer Methods and Programs in Biomedicine*, 103:28–38, 2011.
14. Frangi, A.F., Niessen, W.J., Vincken, K.L., Viergever, M.A. Improvement of retinal blood vessel detection using morphological component analysis. *Proc. of MICCAI*, pages 130–137, 1998.
15. López, A., Lloret, D., Serrat, J., Villanueva, J.J. Multilocal creaseness based on the level set extrinsic curvature. *Comp. Vision and Image Und.*, 77:111–144, 2000.